Cell Metabolism
Article

# Stat3 Activation Links a C/EBPδ to Myostatin Pathway to Stimulate Loss of Muscle Mass

Liping Zhang,[1,5,*] Jenny Pan,[1,5] Yanjun Dong,[1,4] David J. Tweardy,[2] Yanlan Dong,[1] Giacomo Garibotto,[3] and William E. Mitch[1]
[1]Nephrology Division, Department of Medicine
[2]Section of Infectious Diseases, Department of Medicine
Baylor College of Medicine, Houston, TX 77030, USA
[3]Nephrology Division, Department of Internal Medicine, Genoa University, Genoa 16132, Italy
[4]Beijing Institute of Heart, Lung, and Blood Vessel Diseases, An Zhen Hospital Affiliated to Capital Medical University, Beijing 100029, China
[5]These authors contributed equally to this work
*Correspondence: lipingz@bcm.edu
http://dx.doi.org/10.1016/j.cmet.2013.07.012

## SUMMARY

**Catabolic conditions like chronic kidney disease (CKD) cause loss of muscle mass by unclear mechanisms. In muscle biopsies from CKD patients, we found activated Stat3 (p-Stat3) and hypothesized that p-Stat3 initiates muscle wasting. We created mice with muscle-specific knockout (KO) that prevents activation of Stat3. In these mice, losses of body and muscle weights were suppressed in models with CKD or acute diabetes. A small-molecule that inhibits Stat3 activation produced similar responses, suggesting a potential for translation strategies. Using CCAAT/enhancer-binding protein δ (C/EBPδ) KO mice and C2C12 myotubes with knockdown of C/EBPδ or myostatin, we determined that p-Stat3 initiates muscle wasting via C/EBPδ, stimulating myostatin, a negative muscle growth regulator. C/EBPδ KO also improved survival of CKD mice. We verified that p-Stat3, C/EBPδ, and myostatin were increased in muscles of CKD patients. The pathway from p-Stat3 to C/EBPδ to myostatin and muscle wasting could identify therapeutic targets that prevent muscle wasting.**

## INTRODUCTION

Muscle wasting is a debilitating complication of catabolic conditions, including chronic kidney disease (CKD), diabetes, cancer, or serious infections. Unfortunately, there are few reliable strategies that block the loss of muscle protein initiated by these conditions. Previously, we found that myostatin, a negative regulator of muscle growth, is increased in muscles of mice with CKD, and when we inhibited myostatin with a humanized myostatin peptibody, CKD-induced muscle wasting was blocked (Zhang et al., 2011). A similar conclusion was reached in studies of mouse models of cancer cachexia (Zhou et al., 2010). In exploring why blocking myostatin is beneficial for muscle metabolism, we found that its inhibition reduced circulating levels of interleukin-6 (IL-6) and tumor necrosis factor α (TNF-α), suggesting that there is a link between inflammation and muscle wasting as reported in clinical studies (Carrero et al., 2008; Hung et al., 2011). The evidence that inflammation stimulates muscle wasting includes reports that infusion of TNF-α, IL-6, IL-1β, or interferon (IFN)-γ into rodents results in muscle wasting, while neutralization of cytokines using genetic or pharmacological approaches attenuates muscle wasting (Cheung et al., 2010). For example, we treated rodents with a constant infusion of angiotensin II (AngII), which caused muscle wasting plus increased circulating levels of IL-6 and increased expression of suppressor of cytokine signaling 3 (SOCS3), leading to suppressed insulin/insulin-like growth factor 1 (IGF-1) signaling. Knockout IL-6 from mice suppressed AngII-induced muscle wasting (Zhang et al., 2009; Rui et al., 2001; Rui et al., 2002).

Responses to IL-6 or IFN-γ involve stimulation of intracellular signaling pathways, including activation of Janus protein tyrosine kinases (JAKs). Subsequently, JAKs mediate tyrosine phosphorylation of signal transducer and activator of transcription (STAT) factors, followed by their dimerization, nuclear translocation, and activation of target genes (Horvath, 2004). Among the seven members of the STAT family, Stat3 is the major member that is activated by the IL-6 family of cytokines (Hirano et al., 1997; Kishimoto et al., 1994). Recently, Bonetto et al. (2011) reported the results of a microarray analysis of muscles from mice with cancer-induced cachexia. Components of 20 signaling pathways were upregulated, including IL-6, Stat3, JAK-STAT, and SOCS3 complement and coagulation pathways (Bonetto et al., 2011). Although this suggests that the Stat3 pathway could be linked to loss of muscle mass, a pathway from Stat3 to muscle wasting has not been reported.

A potential target of activated Stat3 is CCAAT/enhancer-binding protein δ (C/EBPδ). The C/EBP transcription factors (C/EBPα, -β, -γ, -δ, -ω, and -ζ) are expressed in several tissues and act to regulate inflammatory and metabolic processes (Ramji and Foka, 2002). C/EBPβ or -δ can stimulate intracellular signaling in hepatocytes or inflammatory cells (Poli, 1998; Akira et al., 1990; Alonzi et al., 1997) and in muscles of mice responding to an excess of glucocorticoids, the expression and binding activity of C/EBPβ and -δ are increased (Penner et al., 2002; Yang et al., 2005).

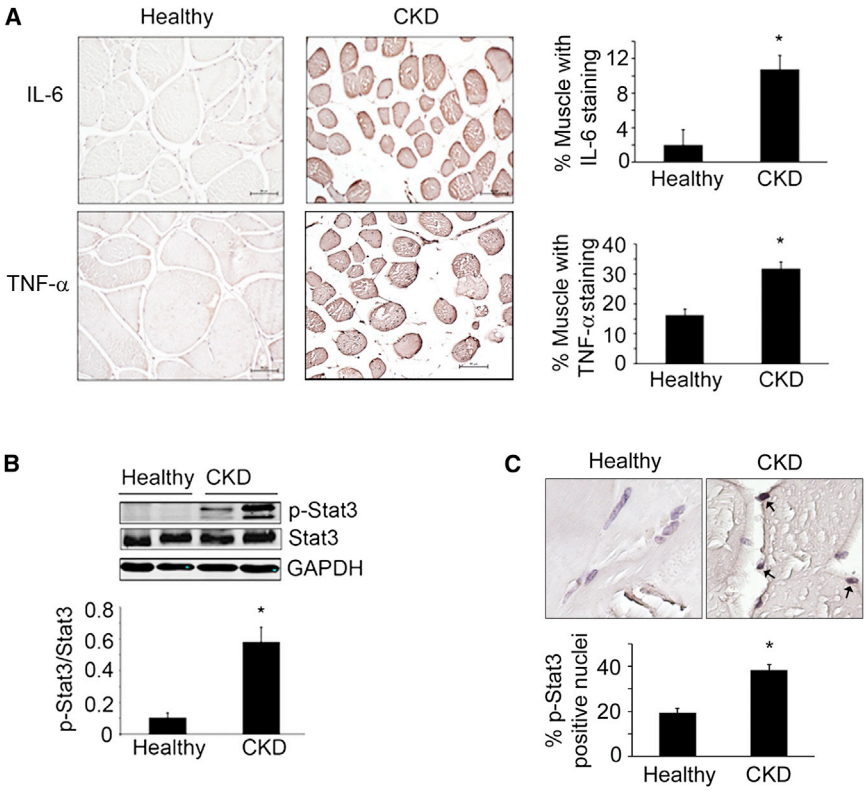


**Figure 1. Inflammatory Cytokines and p-Stat3 Are Elevated in Muscles of Patients with CKD**

(A) Immunostaining of muscle sections for IL-6 and TNF-α (brown color) from biopsies of age- and gender-matched, healthy control subjects (left panel) and CKD patients (middle panel). Staining quantification is calculated as the percentage of muscle fibers that are immunostained (right panel; n = 3 control subjects; n = 4 CKD patients; ruler = 50 μm).

(B) Representative western blots for p-Stat3 in control subjects and CKD patients (upper panel) and the ratio of the intensity of p-Stat3 to total Stat3 (lower panel) (n = 6 control subjects; n = 6 CKD patients).

(C) Muscle sections from control subjects and CKD patients were immunostained for p-Stat3 (upper panel). Brown nuclei are p-Stat3 positive (arrows). Percentage of p-Stat3-positive nuclei in a total of 550 nuclei (lower panel; n = 4 control subjects; n = 6 CKD patients). Values are means ± SEM. *p < 0.05 versus control subjects. See also Figure S1 and Table S1.

A potential mechanism that includes C/EBPδ involves increased myostatin expression because the myostatin promoter contains recognition sites for members of the C/EBP family of transcription factors (Ma et al., 2001; Allen et al., 2010). In the present report, we have uncovered an intracellular signaling pathway in cultured myotubes that could bridge the gaps between p-Stat3 and myostatin and loss of muscle mass. To examine if the pathway was operative in vivo, we studied how two catabolic conditions, CKD or streptozotocin-induced acute diabetes, affected muscle metabolism in a muscle-specific Stat3 knockout (KO) mouse. We also tested whether a small-molecule inhibitor of Stat3 activation would correct muscle wasting. Interruption of Stat3 improved muscle metabolism and strength in mice with CKD. We also found evidence for this catabolic pathway in muscle biopsies from patients with CKD.

## RESULTS

### Muscle Biopsies of Patients with CKD Reveal Inflammation and Stat3 Activation

To address the mechanisms underlying muscle wasting, we studied 18 CKD patients scheduled for peritoneal dialysis catheter insertion and a control group of 16 age- and gender-matched healthy subjects. All subjects led a sedentary lifestyle. In the 18 CKD patients, the blood urea nitrogen (BUN) and serum creatinine were increased 4- and ~8-fold, respectively, over control subjects (Table S1 available online). All CKD patients experienced unintentional weight loss in the 3 months before muscle biopsies were obtained. In CKD patients, the mean estimated protein and calorie intakes were 0.9 g/kg and 28 kcal/kg, respectively, compared to ~1 g/kg and 30–32 kcal/kg, respectively, in control healthy subjects (from diet diaries). Even though these intakes of protein and calorie exceed the recommended daily allowance (RDA), 13 of the 18 patients were malnourished, signified by a subjective global assessment level of >2, and serum albumin was low in 11 patients (<3.8 g/100 ml) (Fouque et al., 2008). Even though the body mass index was low (<23 kg/m$^2$) in only 4 subjects, all patients had evidence of protein losses; there was a marked reduction in muscle fiber cross-sectional area (CSA) (CKD patients median = 1,003 μm$^2$, range 717–1,601; control median = 1,873 μm$^2$, range 1,100–3,389; p < 0.003 Mann-Whitney). We also calculated fat-free mass (FFM) from skinfold thickness (Avesani et al., 2004). Over 3 months, the FFM in CKD patients declined from 45.9 ± 2 kg to 44.1 ± 2 kg (p < 0.05). Regarding drugs that might influence muscle metabolism, no patient was receiving steroids, but 14 patients were treated with statins; these patients did not have signs of myopathy. Characteristics of the CKD patients and control subjects are shown in Table S1. Patients were treated with diuretic (furosemide; all patients) at different dosages, lisinopril or doxazosin (17 patients), proton-pump inhibitors (14 patients), platelet aggregation inhibitors (14 patients), insulin therapy (4 patients), oral anticoagulant therapy (1 patient), and erythropoietin (10 patients). Diabetes was well controlled, with hemoglobin A1c values < 6.5% and fasting plasma glucose levels < 110 mg/dl. There were increased levels of inflammatory markers in CKD patients, including circulating C-reactive protein (CRP; control [3.21 ± 0.22 mg/dl] versus CKD [10.46 ± 2.98 mg/dl]; p < 0.05) and fibrinogen (control [291 ± 31.7 mg/dl] versus CKD [579 ± 37.5 mg/dl]; p < 0.005) (Table S1). There were also increased levels of IL-6 and TNF-α in muscle biopsies compared to results from control subjects (Figure 1A). Finally, TNF-α messenger RNA (mRNA) was increased (Figure S1)

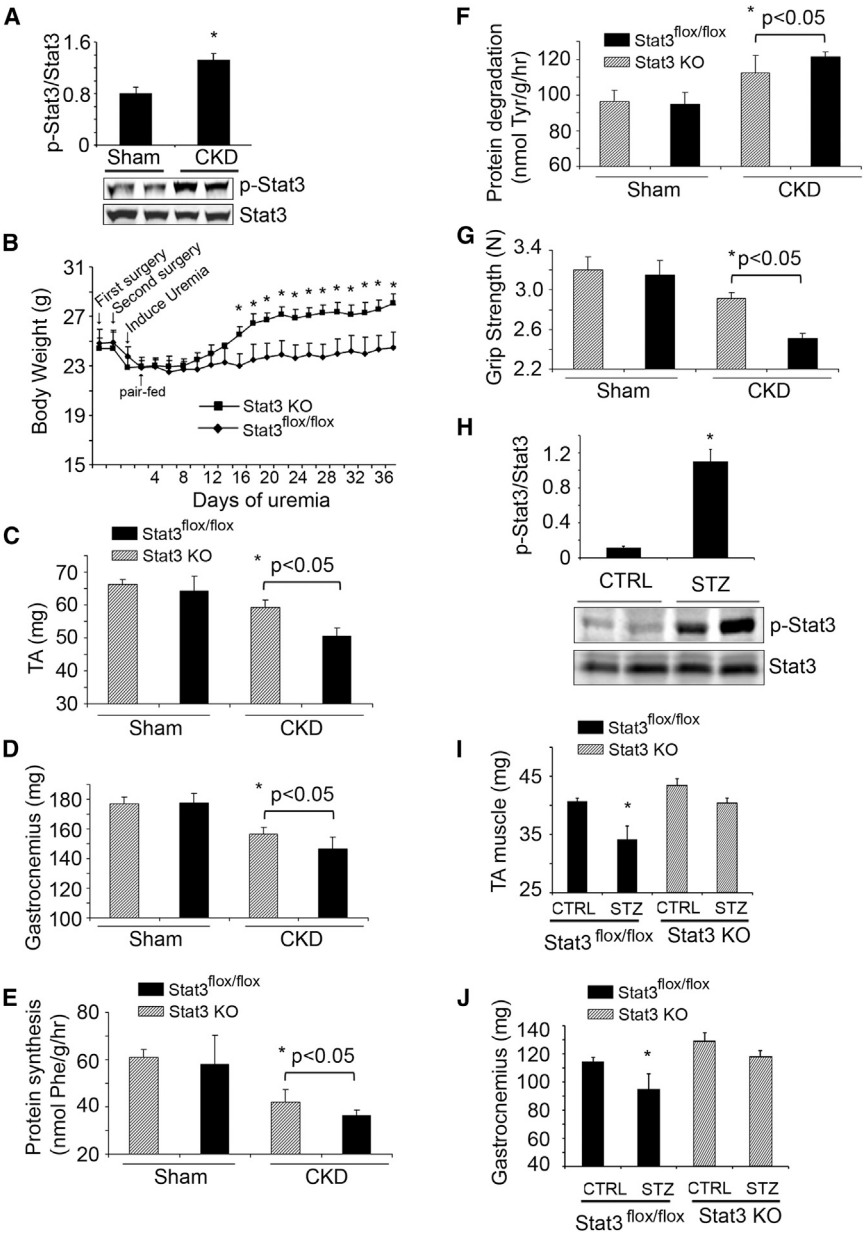


**Figure 2. Muscle-Specific Stat3 Knockout in Mice Suppresses CKD or Streptozotocin-Induced Muscle Wasting**

(A) Density of p-Stat3 corrected for total Stat3 in lysates of gastrocnemius muscles (upper panel; n = 5 mice/group; *p < 0.05 versus sham control mice). Also shown are representative western blots of p-Stat3 (lower panel).

(B) Changes in body weights of Stat3 KO and Stat3$^{flox/flox}$ control mice over 5 weeks following creation of CKD (n = 10 pairs of mice; *p < 0.05 versus Stat3$^{flox/flox}$).

(C and D) Average weights of mixed fiber tibialis anterior (TA) (C) and gastrocnemius (D) muscles (n = 10 mice/group).

(E and F) Extensor digitorum longus (EDL) muscles from sham or CKD mice and either Stat3$^{flox/flox}$ or Stat3 KO were isolated. Rates of protein synthesis (E) and protein degradation (F) were measured (n = 20 EDL muscles from 10 mice/group).

(G) Muscle force of each mouse used in Figure 2B was measured on four consecutive days. The average muscle force (in newtons) is shown (n = 10 mice/group).

(H) Representative western blots of p-Stat3 in lysates of gastrocnemius muscles of acutely diabetic (STZ) and control mice. Bar graph shows the densities of p-Stat3 corrected for that of Stat3 (n = 10 mice/group; *p < 0.05 versus CTRL mice).

(I and J) Average weights of the mixed fiber tibialis anterior (TA) (I) and gastrocnemius (J) muscles from both legs (n = 10 mice/group; *p < 0.05 versus control Stat3$^{flox/flox}$). Values are means ± SEM. See also Figure S2.

and, as noted previously, so was IL-6 mRNA (Verzola et al., 2011).

Activated Stat3 protein was significantly increased in muscles of CKD patients versus healthy subjects (Figure 1B); p-Stat3 was principally located in nuclei of biopsies, as ~40% of nuclei in muscle biopsies of CKD patients were positive for p-Stat3 versus ~20% in healthy subjects (Figure 1C). Thus, significant increases in the expressions of inflammatory cytokines, IL-6 and TNF-α, were associated with Stat3 activation in muscles of CKD patients who expressed evidence of muscle wasting.

## Muscle-Specific Stat3 KO Suppresses Loss of Muscle, Despite CKD or Type 1 Diabetes

In gastrocnemius muscles of mice with CKD, the level of p-Stat3 was increased compared to results in muscles of pair-fed, sham-operated, control mice (Figure 2A). To explore if the activation of Stat3 triggers muscle wasting in vivo, we studied mice with muscle-specific deletion of the Stat3 tyrosine phosphorylation site (Stat3 KO) compared to results in control Stat3$^{flox/flox}$ mice (Takeda et al., 1998). Mice with muscle-specific Stat3 KO did not differ from control mice in terms of development, food intake (data not shown), and body weight (Figure S2A). However, with CKD, body weights of Stat3 KO mice increased versus results in pair-fed Stat3$^{flox/flox}$ mice with CKD (Figure 2B). The gain in weight was due in part to increased muscle mass; after 5 weeks of CKD, the weights of gastrocnemius and tibialis anterior muscles were significantly greater than muscles from Stat3$^{flox/flox}$ mice (Figures 2C and 2D). To determine why loss of muscle mass was blunted in Stat3 KO mice with CKD, we measured rates of muscle protein synthesis and degradation and found a significant improvement in both indices of protein metabolism in Stat3 KO mice with CKD (Figures 2E and 2F). Likewise, there was an increase in grip strength of Stat3 KO mice versus Stat3$^{flox/flox}$ mice (Figure 2G).

Muscle atrophy in several catabolic conditions is characterized as an increase in circulating inflammatory cytokines, impaired insulin/IGF-1 signaling, and an increase in muscle protein

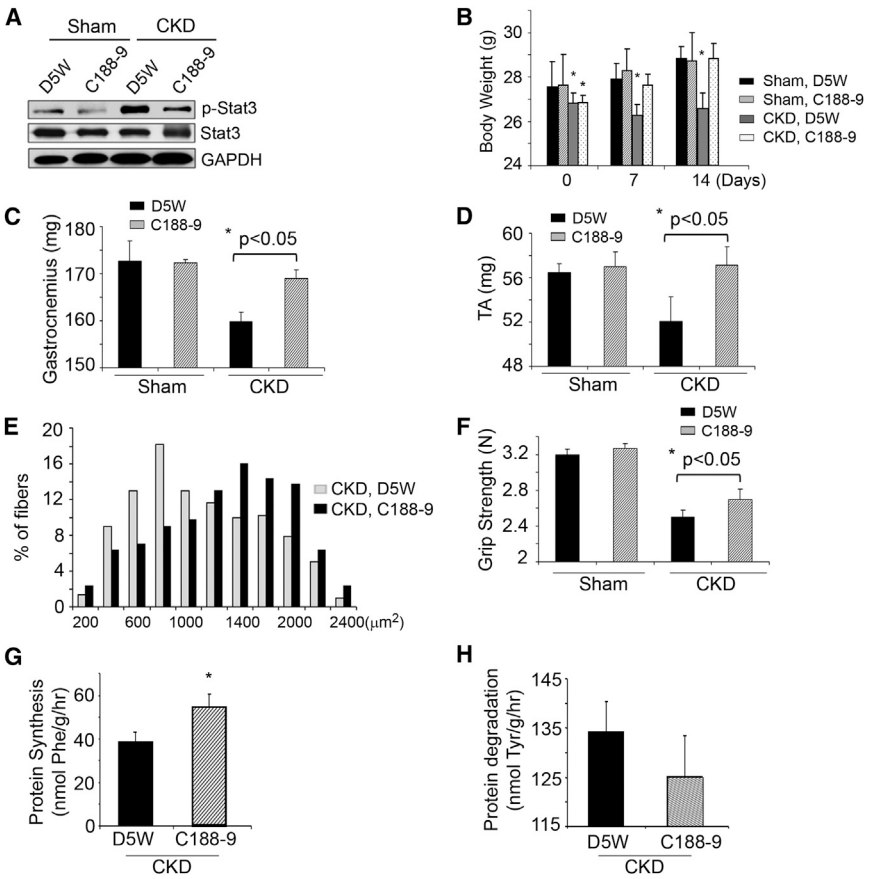


**Figure 3. A Small-Molecule Inhibitor of Stat3 Activation, C188-9, Blocks CKD-Induced Muscle Wasting**

(A) Sham or CKD mice were treated with C188-9 or D5W (diluent) for 14 days. Representative western blots of p-Stat3, Stat3, and GAPDH from lysates of gastrocnemius muscles are shown (n = 8 mice/group).

(B) Differences in body weights of pair-fed, sham, or CKD mice treated with C188-9 or D5W at baseline and after 7 or 14 days of treatment (*p < 0.05 versus D5W sham).

(C and D) Average weights of mixed fiber gastrocnemius (C) and tibialis anterior (TA) (D) muscles from both legs (n = 7 mice/group).

(E) Cryosections of TA muscles were immunostained with anti-laminin to identify the muscle basement membrane. The myofiber areas were measured, and the myofiber size distribution was calculated from the areas of ~500 myofibers assessed by an observer blinded to treatment group (n = 4 pairs of mice).

(F) Muscle force of each mouse studied in Figure 3C was measured on four consecutive days (Experimental Procedures; n = 7 mice/group).

(G and H) At 2 weeks of C188-9 or D5W treatment, protein synthesis (G) and degradation (H) were measured (n = 8 pairs of mice; *p < 0.05 versus D5W). Values are means ± SEM.

degradation via the ubiquitin-proteasome system (UPS) (Zhang et al., 2011; Lecker et al., 2004). To determine if results present in mice with CKD occur in another model of muscle wasting, we studied streptozotocin-treated, acutely diabetic mice (Price et al., 1996). There was an increase in p-Stat3 plus high circulating and muscle levels of IL-6 in acutely diabetic mice (Figures 2H and S2B). IL-6 mRNA in muscles of streptozotocin (STZ)-treated mice was increased 2-fold over control mice (data not shown). Stat3 KO mice expressed a slower decrease in body weight versus results in acutely diabetic $Stat3^{flox/flox}$ mice (Figure S2C). The slower loss of body weight in acutely diabetic Stat3 KO mice was associated with a greater mass of gastrocnemius and tibialis anterior muscles versus results in $Stat3^{flox/flox}$ mice (Figures 2I and 2J). In the absence of CKD- or diabetes-induced catabolism, muscle-specific Stat3 KO did not significantly affect body weight, muscle mass, protein metabolism, or grip strength compared to results in $Stat3^{flox/flox}$ mice (Figure 2). Thus, p-Stat3 can trigger muscle wasting in certain catabolic conditions.

## Inhibition of Stat3 Activation Blocks CKD-Induced Muscle Wasting

To determine if a translational strategy might be developed to interfere with muscle wasting when Stat3 is activated, we evaluated C188-9, a small-molecule inhibitor of Stat3 that targets the phosphotyrosyl (pY) peptide binding pocket within the Src homology (SH) 2 domain of Stat3, thereby blocking Stat3 recruitment to activated receptors, its phosphorylation on tyrosine, and tail-to-tail dimerization (Xu et al., 2009; Redell et al., 2011). After 2 weeks of CKD, mice were paired for their BUN and body weights and injected with either C188-9 or the diluent, 5% dextrose in water (D5W). C188-9 treatment decreased the level of p-Stat3 in muscle without affecting levels of total Stat3 (Figure 3A). Consistent with results from Stat3 KO mice with CKD, the body weights of CKD mice treated with the Stat3 inhibitor were significantly greater than weights of the control, CKD mice (Figure 3B). After 14 days of C188-9, we found that the increase in body weight included more muscle, as the weights of gastrocnemius and tibialis anterior muscles were greater (Figures 3C and 3D). The increase in muscle mass was confirmed by an analysis of the size distribution of myofibers in muscles of CKD mice treated with C188-9 (Figure 3E). This improvement in muscle mass was accompanied by improved grip strength in CKD mice treated with C188-9 (Figure 3F). Consistent with results from the Stat3 KO mice, blocking Stat3 with C188-9 in control, wild-type mice did not significantly affect their food intake (data not shown), body weight, muscle mass, or grip strength (Figures 3B–3D and 3F). The mechanism underlying the C188-9-induced increase in muscle weight included improved muscle protein synthesis and decreased protein degradation (Figures 3G and 3H). We conclude that inhibiting Stat3 activation suppresses CKD-induced loss of both muscle mass and strength.

## In C2C12 Myotubes, Stat3 Activation Increases the Expression of C/EBPδ and Myostatin

We evaluated the signaling pathway from activated Stat3 to muscle wasting. We studied myostatin because its expression

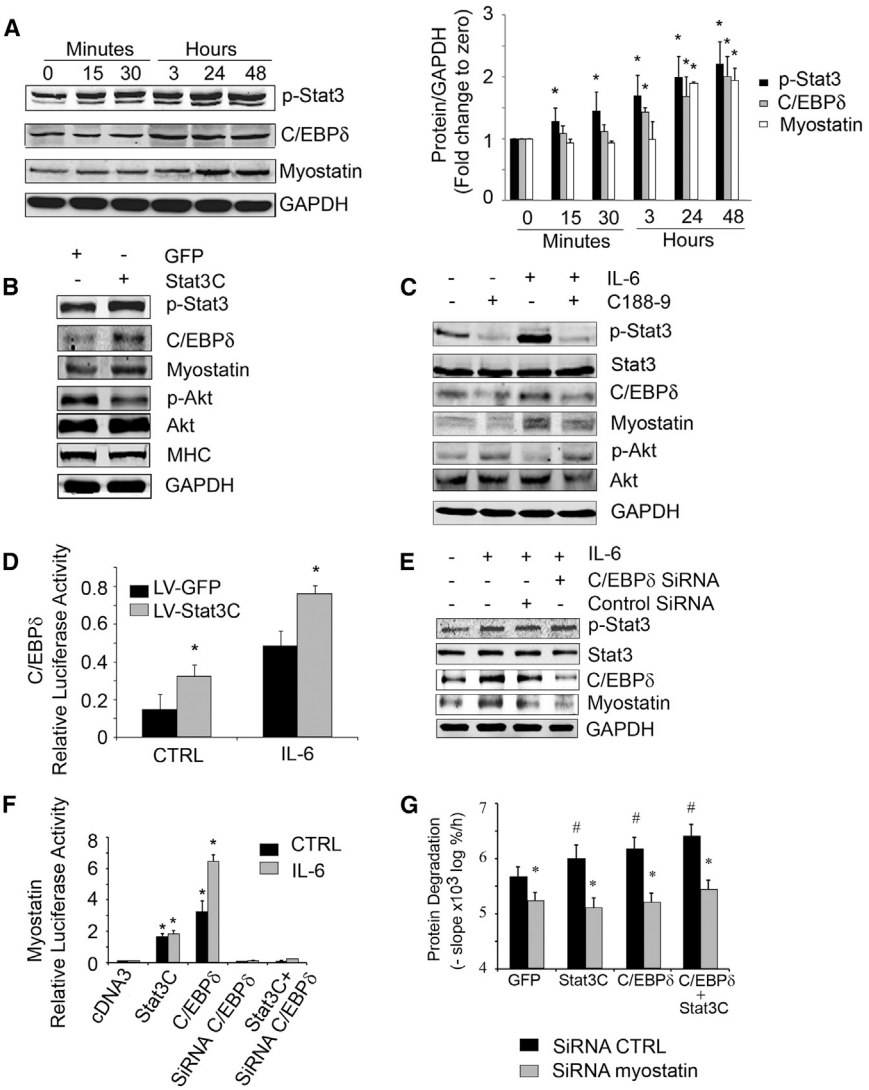


**Figure 4. Stat3 Activation in C2C12 Myotubes Increases the Expression of C/EBPδ and Myostatin**

(A) Representative western blots from C2C12 myotubes treated with IL-6 (100 ng/ml) for different times (left panel). Fold changes in the densities of proteins corrected for GAPDH at different times was calculated from values at time zero (right panel), n = 3 repeats; *p < 0.05 versus time zero.

(B) C2C12 myotubes were infected with a lentivirus expressing constitutively active Stat3 (Stat3C-GFP). A representative western blot for the indicated proteins is shown.

(C) C2C12 myotubes were treated with or without C188-9 for 2 hr before adding IL-6 (100 ng/ml) for 24 hr. A representative western blot for the indicated proteins is shown.

(D) C2C12 myoblasts were cotransfected with a plasmid expressing the C/EBPδ promoter-driven luciferase and a plasmid expressing *Renilla* luciferase. A lentivirus expressing Stat3C-GFP was also transfected into the cell myoblasts. The cells were treated with or without IL-6. Dual luciferase activity was measured (n = 3 repeats; *p < 0.05 versus respective GFP control).

(E) C2C12 myoblasts were transfected with control siRNA or C/EBPδ siRNA and, after differentiation to myotubes, were treated with or without IL-6. Representative western blots of Stat3, C/EBPδ, and myostatin are shown.

(F) C2C12 myoblasts were cotransfected with a plasmid expressing the myostatin promoter-driven luciferase plus plasmids (cDNA3 control, Stat3C, C/EBPδ, C/EBPδ siRNA, or Stat3C plus C/EBPδ siRNA) and treated with or without IL-6. Luciferase activity was measured (n = 3 repeats; *p < 0.05 versus cDNA3 CTRL).

(G) C2C12 myoblasts were transfected with lentivirus expressing a siRNA to myostatin. Myoblasts exhibiting suppression of myostatin were selected and then differentiated after they had been transfected with plasmids expressing Stat3C, C/EBPδ, or Stat3C plus C/EBPδ. In these cells, we measured protein degradation (upper panel; n = 6 repeats, #p < 0.05 versus GFP control, *p < 0.05 versus siRNA CTRL). Western blots of proteins expressed in response to transfections were shown in Figure S3E. Values are means ± SEM. See also Figure S3.

is increased in muscles of CKD mice, and we have found that myostatin inhibition overcomes the decrease in protein synthesis and the increase in protein degradation stimulated by CKD (Zhang et al., 2011). To determine how CKD leads to myostatin expression, we evaluated C/EBPδ because the myostatin promoter has several C/EBP recognition sites (Ma et al., 2001) and Stat3 can regulate C/EBPδ, at least in epithelial cells (Zhang et al., 2007). First, we treated C2C12 myotubes with IL-6 to activate Stat3. After 3 hr, there was an increase in the C/EBPδ protein in myotubes responding to activated Stat3. After 24 hr, myostatin protein was increased, and changes in mRNAs were consistent with the western blotting results (Figures 4A, S3A, and S3B). These results show that p-Stat3, C/EBPδ, and myostatin were activated sequentially.

Next, we infected C2C12 myotubes with a lentivirus that expresses a constitutively active Stat3-GFP (Stat3C-GFP). The higher level of p-Stat3 expression resulted in an increase in C/EBPδ and myostatin plus a decrease in p-Akt and myosin heavy chain (MHC) as compared to results from myotubes expressing GFP alone (Figure 4B). Other evidence that Stat3 activation stimulates myostatin expression was uncovered when we used the inhibitor of Stat3 (C188-9) to block p-Stat3 in C2C12 myotubes. After 24 hr of exposure to IL-6, there was an increase in p-Stat3, C/EBPδ, and myostatin, and C188-9 blocked these responses. The inhibitor also increased p-Akt (Figure 4C) and suppressed C/EBPδ and myostatin mRNAs in IL-6-treated C2C12 myotubes (Figure S3C). Notably, C188-9 not only suppressed p-Stat3, but also prevented the decrease in myotube size induced by exposure to IL-6 (Figure S3D).

To assess whether Stat3 affects C/EBPδ expression, we cotransfected C2C12 myoblasts with a plasmid expressing a C/EBPδ promoter-driven luciferase plus a lentivirus expressing the constitutively active Stat3C-GFP. Overexpression of Stat3C increased C/EBPδ promoter activity compared to that in

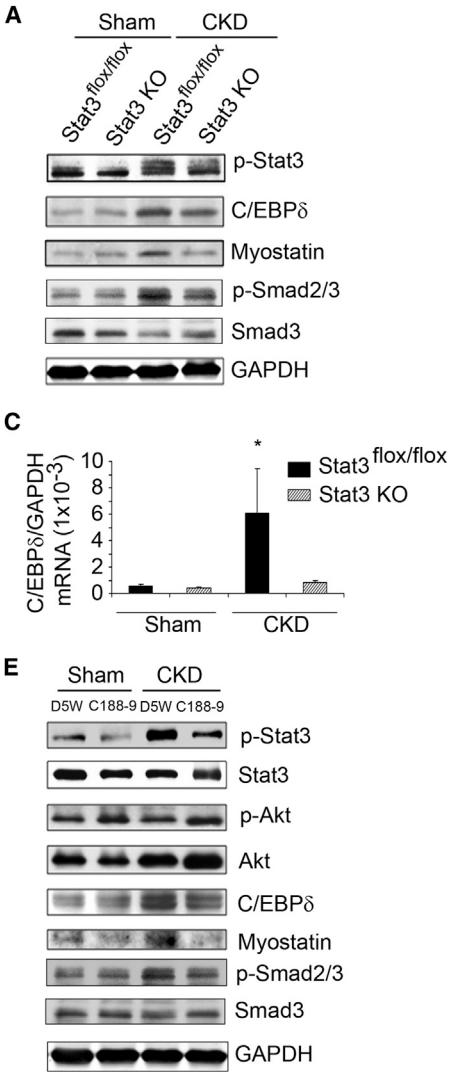


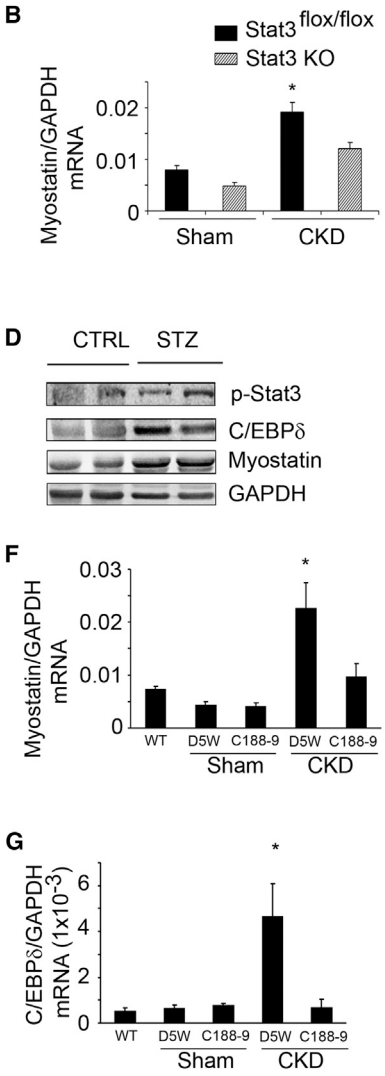


**Figure 5. Stat3 Activation in Mouse Muscles Increases C/EBPδ and Myostatin Expression**

(A) Representative western blots of the indicated proteins from lysates of gastrocnemius muscles of control (Stat3$^{flox/flox}$) or Stat3 KO sham or CKD mice.

(B and C) mRNAs of myostatin (B) and C/EBPδ (C) in muscles of sham or CKD mice analyzed by RT-PCR (n = 4 mice/group; *p < 0.05 versus Stat3$^{flox/flox}$ sham).

(D) Representative western blots of the indicated proteins in lysates of gastrocnemius muscles of STZ versus WT control mice (n = 5 pairs).

(E) Sham or CKD mice were treated with C188-9 or D5W (diluent) for 14 days. Representative western blots of indicated proteins from lysates of gastrocnemius muscles are shown (n = 8 mice/group).

(F and G) mRNA levels of myostatin (F) and C/EBPδ (G) analyzed by RT-PCR and corrected for GAPDH (n = 3 mice/group: wild-type mice without CKD; sham mice treated with C188-9 or D5W; mice with CKD treated with C188-9 or D5W; *p < 0.05 versus WT non-CKD). Values are means ± SEM.

lentivirus expressing GFP control; addition of IL-6 stimulated C/EBPδ promoter activity in myoblasts (Figure 4D).

To identify whether p-Stat3 acts through C/EBPδ to stimulate myostatin, we knocked down C/EBPδ using small interfering RNA (siRNA). In this case, the IL-6-induced increase in myostatin expression was blocked when C/EBPδ was suppressed, even though p-Stat3 was increased (Figure 4E). Next, we cotransfected C2C12 myoblasts with a plasmid expressing myostatin promoter-driven luciferase plus one of the following: (1) a plasmid expressing Stat3C; (2) a plasmid expressing C/EBPδ; (3) C/EBPδ siRNA oligonucleotide; or (4) a plasmid expressing Stat3C and the C/EBPδ siRNA. Constitutively active Stat3C moderately increased myostatin promoter activity, while transfection with C/EBPδ alone significantly increased myostatin promoter activity. Knockdown of C/EBPδ blocked myostatin promoter activity that was stimulated by IL-6 or Stat3C (Figure 4F).

We also tranfected C2C12 myoblasts with a lentivirus that expresses myostatin siRNA; it decreased myostatin expression and reduced protein degradation even in cells expressing Stat3C or C/EBPδ (Figures 4G and S3E). Thus, the Stat3 to C/EBPδ to myostatin pathway provides a mechanism causing loss of muscle mass.

## CKD-Induced Muscle Wasting In Vivo Is Mediated by a Pathway from p-Stat3 to C/EBPδ to Myostatin

In muscles of CKD or acutely diabetic mice, there were increases in the expression of p-Stat3, C/EBPδ, and myostatin (Figures 5A and 5D). The C/EBPδ and myostatin proteins in muscles of Stat3 KO mice with CKD were significantly below responses in muscles of Stat3$^{flox/flox}$ mice with CKD. Expression of p-Smad2 and p-Smad3, the downstream signal of myostatin, was also increased in muscles of CKD mice, consistent with reports that p-Smad2 and p-Smad3 mediates myostatin-induced muscle atrophy (Trendelenburg et al., 2009). We note that the increase in p-Smad2 and p-Smad3 in muscle of mice with CKD was sharply decreased in muscles of Stat3 KO mice with CKD. This suggests that in CKD, Stat3 activation results in myostatin expression and activation of its downstream signaling pathway (Figure 5A). Similar results were found when we examined C/EBPδ and myostatin mRNAs in muscles of the Stat3 KO mice with CKD; levels in Stat3 KO mice with CKD were below those of control, Stat3$^{flox/flox}$ mice with CKD (Figures 5B and 5C). We also note that activated Stat3 in muscles of CKD mice was not completely blocked by muscle-specific KO of Stat3 when compared to p-Stat3 in muscles of non-CKD mice. Possibly, the remaining p-Stat3 in muscle lysates of Stat3 KO mice could reflect p-Stat3 in blood cells, blood vessels, or the interstitium since the results were obtained from western blots of gastrocnemius muscle lysates.

When we treated mice with CKD using the inhibitor of Stat3, both C/EBPδ and myostatin proteins were decreased, and the CKD-induced phosphorylation of p-Smad2 and p-Smad3 was blocked. In this case, the Akt phosphorylation was higher (Figure 5E). Notably, C188-9 suppressed the CKD-stimulated mRNA expressions of C/EBPδ and myostatin (Figures 5F and 5G). In control mice without CKD, muscle-specific Stat3 KO or C188-9 treatment did not change either C/EBPδ or myostatin mRNAs or proteins in muscle.

To demonstrate a link from p-Stat3 to C/EBPδ to myostatin in vivo, we studied C/EBPδ-deficient mice that have normal embryonic development, are fertile, and do not display overt developmental or physiological defects (Sterneck et al., 1998). We created CKD in heterozygous and homozygous C/EBPδ KO and wild-type mice and fed the different groups the same amount of chow as eaten by wild-type mice with CKD. In homozygous C/EBPδ KO mice with CKD, the losses of body and muscle weights were prevented. There was also improved survival in pair fed, homozygous C/EBPδ KO mice with CKD (Figures 6A–6C). Despite the increase in p-Stat3 in muscles of homo- and heterozygous C/EBPδ KO or wild-type mice with CKD, there was no increase in expression of myostatin in mice with homozygous C/EBPδ KO (Figure 6D). The degrees of survival and myostatin expression in muscles of heterozygous C/EBPδ KO mice were intermediate between homozygous KO and wild-type mice.

To examine whether Stat3-induced muscle wasting in vivo is mediated by myostatin, we injected a lentivirus expressing constitutively active Stat3-GFP (Stat3C-GFP) into the right hindlimb of newborn mice. The injection was repeated 2 weeks later. At the same time, a lentivirus expressing GFP was injected into the left hindlimb (control). At 2 weeks after the second injection of lentiviruses into hindlimbs, one group of mice was injected with anti-myostatin peptibody for 2 weeks and compared to mice injected with PBS (Figure 6E). In mice treated with PBS, the overexpression of Stat3C induced a significant reduction in myofiber sizes versus results in the contralateral hindlimb, which was injected with GFP (Figure 6F; compare bar 2 with bar 1). Notably, myostatin inhibition slightly increased the sizes of myofibers in muscles treated with GFP alone (Figure 6F; compare bar 3 with bar 1). Myostatin inhibition also eliminated the myofiber atrophy induced by Stat3C: there was no difference in myofiber sizes in muscles expressing GFP versus Stat3C-GFP (Figure 6F; compare bar 3 with bar 4). Next, we immunostained muscle cross-sections with p-Smad2 and p-Smad3 and found high levels of p-Smad2 and p-Smad3 in myofibers overexpressing Stat3C-GFP. Similar to results in CKD mice with muscle-specific Stat3 KO or following treatment with the Stat3 inhibitor, the increase in p-Smad2 and p-Smad3 was blocked by the anti-myostatin peptibody (Figures 6E, 6G, and S4), consistent with a catabolic pathway from p-Stat3 to C/EBPδ to myostatin-induced muscle protein loss.

### In CKD Patients, There Is Evidence for the p-Stat3 to C/EBPδ to Myostatin Pathway in Muscle

Muscle biopsies from patients with advanced CKD had significantly decreased sizes of myofibers and levels of p-Akt (Table S1; Figure 7A). There was, however, increased mRNA and protein levels of p-Stat3, C/EBPδ, and myostatin in muscles of CKD patients (Figures 7B–7D).

## DISCUSSION

Many catabolic conditions, including CKD, diabetes, cancer, and serious infections, are complicated by progressive muscle wasting, which decreases the quality of life and raises the risk of morbidity and mortality. The complications of CKD (excess angiotensin II, glucocorticoids, acidosis, and impaired insulin/IGF-1 signaling) stimulate protein degradation and loss of muscle mass. CKD also increases inflammatory markers, including IL-6, TNF-α, and CRP, which can activate p-Stat3 (Zhang et al., 2009, 2011; May et al., 1987; Hu et al., 2009). Still, the molecular mechanisms causing muscle loss are poorly understood, which hampers the development of drug or other treatment strategies. In the present experiments, we have identified that activated Stat3 triggers a pathway from p-Stat3 to myostatin, which causes the progressive muscle wasting that is induced by CKD or acute diabetes.

Evidence for the p-Stat3-dependent pathway that initiates loss of muscle mass was obtained in five experimental models: cultured C2C12 myotubes; muscle-specific p-Stat3 KO mice; mice treated with a small molecule that inhibits Stat3 activation; C/EBPδ KO mice; and muscle biopsies of patients with CKD. Our results show that CKD activates Stat3, leading to increased expression of C/EBPδ and transcriptional regulation of myostatin expression. When this pathway is activated, there is a decrease in p-Akt, which we have shown will activate caspase-3 and the ubiquitin-proteasome system (UPS) to degrade muscle protein (Zhang et al., 2011; Du et al., 2004; Wang et al., 2010). Our results demonstrate that: (1) CKD or acute diabetes activates Stat3 in muscle, causing loss of muscle mass; (2) targeted knockout of Stat3 in muscle or pharmacologic inhibition of Stat3 suppresses the muscle wasting that is induced by CKD or acute diabetes, which leads to an increase in muscle protein synthesis and a decrease in protein degradation with improvement in muscle mass and grip strength; and (3) C/EBPδ is a mediator of the pathway from p-Stat3 to myostatin because its KO inhibits myostatin expression and suppresses muscle wasting. In addition, C/EBPδ KO was associated with an improvement in survival. In muscle biopsies of patients with CKD, there are similar changes in the levels of the same mediators, suggesting that the results could form the basis for developing translation strategies to suppress muscle wasting in CKD.

Presently, there are no clinically available drugs that directly target Stat3. We initiated a small-molecule, drug development program that targets the pY-peptide binding site within the Stat3 SH2 domain and identified C188 (Xu et al., 2009); further hit-to-led development yielded C188-9 (Redell et al., 2011). C188-9 blocks Stat3 binding to its pY-peptide ligand with $K_i$ = 136 nM; C188-9 does not inhibit upstream JAK or Src kinases (Redell et al., 2011) and is well tolerated in mice even after prolonged administration. Results obtained using C188-9 in our mouse CKD cachexia model suggest that it has promise for development into a drug that can be administered safely to treat or prevent cachexia in patients.

How does C188-9 influence muscle protein wasting? One possibility is suggested by the findings that injection of IL-6 into rodents activates Stat3 and stimulates muscle proteolysis (Goodman, 1994). Indeed, we found increased IL-6 in muscles of CKD patients and in STZ-induced acute diabetic mice. The

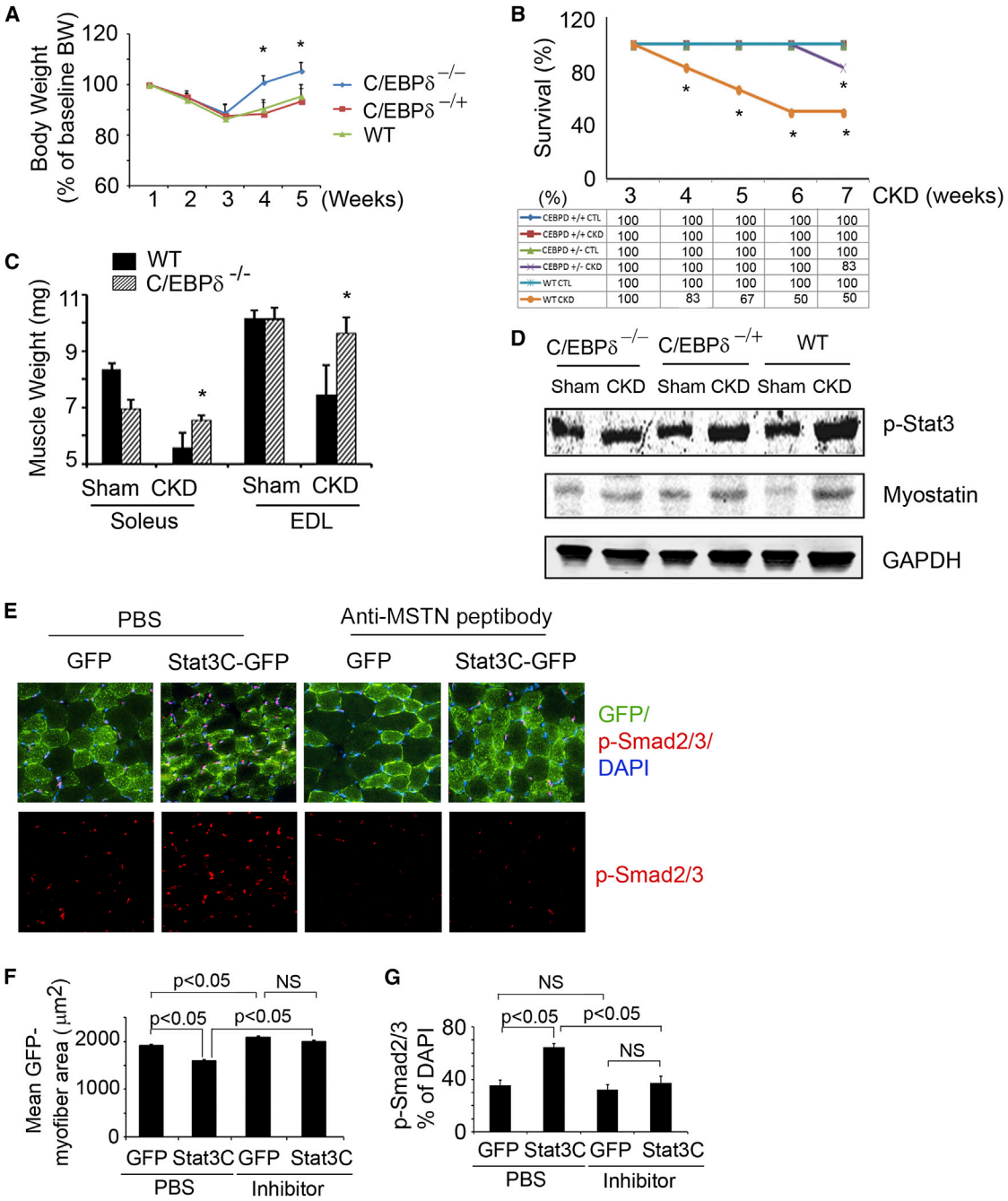


**Figure 6. C/EBPδ and Myostatin Mediate CKD or Stat3-Induced Muscle Wasting**

(A) Body weights of wild-type or homo- or hetero-C/EBPδ KO mice following creation of CKD. Values are expressed as a percentage of basal body weight (mean ± SEM; n = 9 for WT mice; n = 11 for C/EBPδ$^{-/-}$; n = 11 for C/EBPδ $^{-/+}$ mice; *p < 0.05 versus WT CKD).

(B) Survival was calculated as the percentage of mice surviving at 3 weeks after CKD or after sham surgery (n = 20 for WT; n = 25 for C/EBPδ$^{-/-}$; n = 21 for C/EBPδ$^{+/-}$; *p < 0.05 versus C/EBPδ$^{-/-}$ CKD).

(C) Average weights from both legs of red fiber (soleus) or white fiber (EDL) muscles (n = 10 mice/group; *p < 0.05 versus WT CKD).

(D) Representative western blots of p-Stat3 and myostatin from muscles of CKD or sham-operated mice of the following groups: C/EBPδ$^{-/-}$, C/EBPδ$^{-/+}$, or control (WT).

(E) Cryosections of gastrocnemius muscles from mice that were transfected with lentivirus-expressing Stat3C-GPF or GFP and treated with anti-myostatin inhibitor or PBS. The sections were immunostained with p-Smad2 and p-Smad3 (red, lower panel). The overlap picture (upper panel) shows GFP-positive myofibers (green) that expressed p-Smad2 and p-Smad3.

(F) GFP-positive areas in myofibers (Figure 6E) were measured, and the mean myofiber sizes of each group are shown.

(G) The percentage of p-Smad2- and p-Smad3-positive nuclei to total nuclei was calculated. Values are means ± SEM. See also Figure S4.

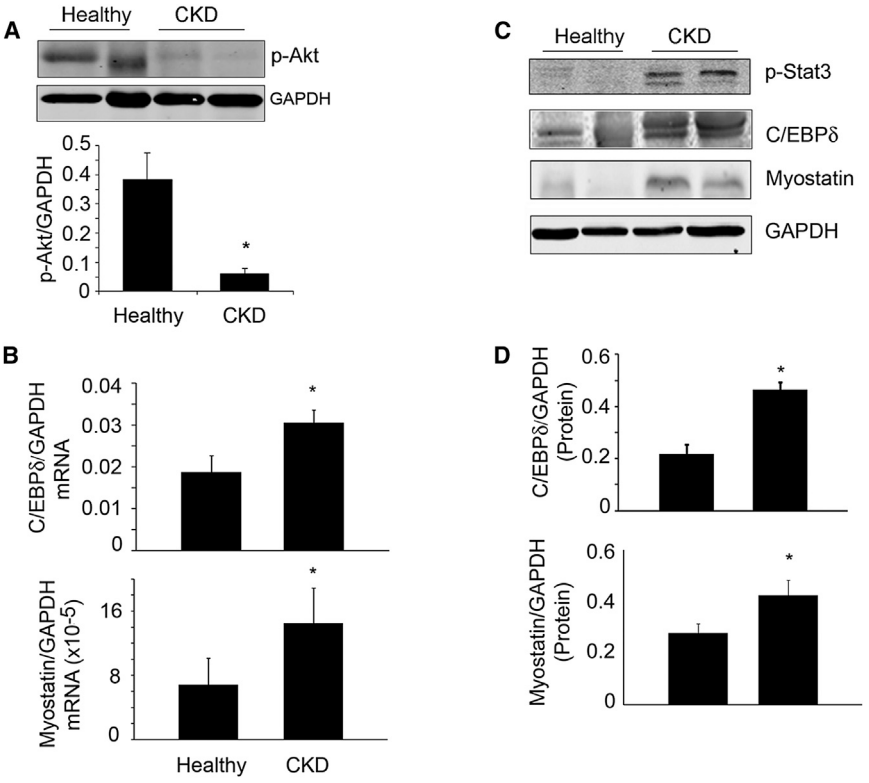


**Figure 7. Evidence for a p-Stat3, C/EBPδ, and Myostatin Pathway in Muscles of Patients with CKD**

(A) Representative western blots of p-Akt from muscle biopsies of healthy control or CKD patients. Bar graph shows the densities of p-Akt corrected for GAPDH (lower panel; n = 4 CKD patients and 3 healthy subjects).

(B) Levels of mRNAs of C/EBPδ or myostatin were analyzed by RT-PCR from muscle biopsies of healthy control or CKD patients (n = 5 control subjects and 9 CKD patients).

(C) Representative western blots of the indicated proteins from muscle biopsies from healthy control or CKD patients.

(D) The band densities in (C) were quantified after correction for GAPDH (n = 3 pairs for CEBPδ; n = 8 pairs for myostatin). Values are means ± SEM. *p < 0.05 versus healthy controls.

latter is consistent with reports from type 1 diabetic patients (Myśliwiec et al., 2006; Myśliwiec et al., 2008; Shelbaya et al., 2012). The potential origin of IL-6 in type 1 diabetes includes peripheral blood mononuclear cells and/or T helper 17 (Th17) cells (Bradshaw et al., 2009; Foss-Freitas et al., 2006; Ryba-Stanisławowska et al., 2013). However, others find that IL-6 does not stimulate muscle loss in the absence of another illness, such as cancer (Baltgalvis et al., 2008). Thus, it is unclear how cytokines cause muscle proteolysis. We propose that the increase in IL-6 stimulated by CKD (Kimmel et al., 1998), and possibly other cytokines, activates p-Stat3, which triggers muscle wasting. Indeed, when we deleted Stat3 from muscle or when we studied the Stat3 inhibitor, C188-9, CKD-induced muscle wasting was inhibited. How could p-Stat3 stimulate muscle wasting? We have demonstrated that p-Stat3 upregulates C/EBPδ and increases the transcription of myostatin, a potent negative regulator of muscle mass. Others have implicated C/EBPδ in the pathogenesis of catabolic disorders. For example, based on microarray analyses, there was upregulation of multiple genes, including C/EBPδ in muscles of mice with cancer cachexia or in muscle biopsies of hemodialysis patients (Bonetto et al., 2011; Gutiérrez et al., 2008). In addition, there are reports that p-Stat3 stimulates C/EBPδ expression in cancer, immune, or liver cells. This is relevant because the C/EBPδ promoter contains a Stat3 binding site, making it a likely participant in the pathway (Zhang et al., 2007; Sanford and DeWille, 2005). Indeed, we found that exposure of C2C12 myotubes to IL-6 stimulates p-Stat3 and sequentially increases the expression of C/EBPδ. Likewise, expression of constitutively active Stat3 in myotubes increased C/EBPδ promoter activity and the expression of C/EBPδ protein. Conversely, Stat3 inhibition in C2C12 myotubes or in CKD mice suppressed the expression of C/EBPδ. A likely target of C/EBPδ is myostatin. For example, when we knockdown C/EBPδ by siRNA in myotubes, the increase in myostatin stimulated by IL-6 was blocked. In addition, knockout of C/EBPδ in mice with CKD prevented their loss of muscle mass and expression of myostatin. These results are consistent with reports that myostatin is expressed in a wide variety of catabolic conditions associated with muscle wasting, including cancer, CKD, diabetes, or weightlessness (spaceflight) (Zhou et al., 2010; Zhang et al., 2011; Feldman et al., 2006; Lalani et al., 2000). In mice with CKD, the activation of Stat3 leads to expression of myostatin and its downstream signals, p-Smad2 and p-Smad3, plus accelerated protein degradation. Overexpression of Stat3C in muscle of mice causes a decrease in myofiber sizes; knocking down myostatin resolves the phenotype of Stat3 activation because myofiber sizes are increased and p-Smad2 and p-Smad3 levels are reduced. Our results that Stat3 induces myostatin expression could apply to other members of the TGF-β superfamily, such as Activin A. Lipopolysaccharides and cytokines, including IL-6 and IL-1β, induce expression of Activin A (Okuma et al., 2005); high levels of Activin A have been shown to induce muscle atrophy (Zhou et al., 2010). Importantly, treatment of mice with cancer-induced cachexia using a soluble Activin A receptor (actRIIB) blocked the loss of muscle mass (Zhou et al., 2010). Additional studies will be necessary to determine if Activin A induction by cytokines is mediated through Stat3.

The mechanism by which an increase in myostatin leads to loss of muscle mass could be a decrease in p-Akt in muscle. A decrease in p-Akt activates caspase-3, leading to cleavage of the complex structure of muscle proteins and activation of proteolysis by the 26S proteasome (Du et al., 2004; Wang et al., 2010). In addition, a low p-Akt level would reduce phosphorylation of forkhead transcription factors, which stimulate the expression of the muscle-specific E3 ubiquitin ligases, Atrogin-1/MAFbx or MuRF-1, and accelerate proteolysis in the UPS

(Sandri et al., 2004; Lee et al., 2004; Stitt et al., 2004; Lecker et al., 2006). In the present experiments, inhibition of p-Stat3 with C188-9 decreased myostatin expression and the activation of its downstream signaling mediators, p-Smad2 and p-Smad3; there also was an increase in p-Akt. There was also a sharp decrease in p-Akt in muscle of CKD patients, with increased mRNA and protein expressions of C/EBPδ and myostatin.

In summary, our results have uncovered a pathway that stimulates muscle wasting in response to activation of Stat3. The pathway is activated by CKD or acute diabetes and provides insights into the relationships among the signaling molecules, Stat3, C/EBPδ, and myostatin. Results from our studies of cultured skeletal muscle cells or mice are consistent with changes in the levels of the same signaling molecules in muscle biopsies of CKD patients. Consequently, these results might be translated into treatment strategies for catabolic conditions like CKD that cause muscle wasting. Development of a safe and potent small-molecule Stat3 inhibitor may represent a therapeutic approach to muscle wasting in catabolic conditions.

## EXPERIMENTAL PROCEDURES

### Mouse Models

All animal experiments and procedures were approved by the Baylor College of Medicine Institutional Animal Care and Use Committee (IACUC). Subtotal nephrectomy was used to create CKD in mice (Zhang et al., 2011; May et al., 1987). To induce diabetes, we injected 12-week-old $Stat3^{flox/flox}$ and Stat3 KO mice intraperitoneally with 2 doses of 150 mg/kg/d STZ (Sigma-Aldrich) in 0.1 M citrate buffer (pH 4). Control mice were injected with the citrate buffer. Mice were housed in individual cages, and the diabetic $Stat3^{flox/flox}$ mice were pair-fed with diabetic Stat3 KO mice for 9 days.

### Muscle Biopsies

During placement of a peritoneal dialysis catheter in CKD patients, the rectus abdominis muscle was biopsied, frozen at −80°C, and stored until analyzed. Biopsy of this muscle was obtained from healthy subjects during abdominal hernia surgeries. The procedures were approved by the Ethical Committee of the Department of Internal Medicine of the University of Genoa, in accordance with the Helsinki declaration regarding ethics of human research.

### mRNA Analyses

mRNAs were analyzed by RT-PCR as described (Takeda et al., 1998). Primers are listed in Table S2. Relative mRNA levels were calculated from cycle threshold (Ct) values using glyceraldehyde 3-phosphate dehydrogenase (GAPDH) as the internal control (relative expression = $2^{[\text{sample Ct} - \text{GAPDH Ct}]}$). See Table S2 for primer sequences.

### Muscle Force Measurement

Mouse grip strength was measured daily for 4 consecutive days using a Grip Strength Meter (Columbus Instruments). Each day, 5 grip strengths were assessed at 1 min intervals, and the average grip strength over 4 days was calculated.

### Statistical Analysis

Data were expressed as the mean ± SEM. Differences between two groups were analyzed by the t test; multiple comparisons were analyzed by ANOVA with a post hoc analysis by the Student-Newman-Keuls test for multiple comparisons. Results were considered statistically significant at $p < 0.05$.

## SUPPLEMENTAL INFORMATION

Supplemental Information includes Supplemental Experimental Procedures, four figures, and two tables and can be found with this article online at http://dx.doi.org/10.1016/j.cmet.2013.07.012.

## ACKNOWLEDGMENTS

These experiments were supported by the generous support of Dr. and Mrs. Harold Selzman, grants from the Norman S. Coplon Extramural Research Foundation and the American Diabetic Association to L.Z., NIH Grants R37-DK37175 and T32-DK62706 to W.E.M., and NIH grants R21-CA149783 and R41-CA153658 and grant RP100421from the Cancer Prevention and Research Institute of Texas to D.J.T. G.G. is supported by grants from the Ministero dell'Università e della Ricerca Scientifica e Tecnologica and from Genoa University. The authors thank Dr. E. Sterneck (NIH-NCI, Fredericksburg, MD) for the C/EBPδ knockout mice and the C/EBPδ promoter-luciferase reporter construct. Dr. D. Allen (University of Colorado) kindly provided the myostatin promoter-luciferase reporter construct.

Received: April 9, 2012
Revised: March 17, 2013
Accepted: July 24, 2013
Published: September 3, 2013

## REFERENCES

Akira, S., Isshiki, H., Sugita, T., Tanabe, O., Kinoshita, S., Nishio, Y., Nakajima, T., Hirano, T., and Kishimoto, T. (1990). A nuclear factor for IL-6 expression (NF-IL6) is a member of a C/EBP family. EMBO J. *9*, 1897–1906.

Allen, D.L., Cleary, A.S., Hanson, A.M., Lindsay, S.F., and Reed, J.M. (2010). CCAAT/enhancer binding protein-delta expression is increased in fast skeletal muscle by food deprivation and regulates myostatin transcription in vitro. Am. J. Physiol. Regul. Integr. Comp. Physiol. *299*, R1592–R1601.

Alonzi, T., Gorgoni, B., Screpanti, I., Gulino, A., and Poli, V. (1997). Interleukin-6 and CAAT/enhancer binding protein beta-deficient mice act as tools to dissect the IL-6 signalling pathway and IL-6 regulation. Immunobiology *198*, 144–156.

Avesani, C.M., Draibe, S.A., Kamimura, M.A., Dalboni, M.A., Colugnati, F.A., and Cuppari, L. (2004). Decreased resting energy expenditure in non-dialysed chronic kidney disease patients. Nephrol. Dial. Transplant. *19*, 3091–3097.

Baltgalvis, K.A., Berger, F.G., Pena, M.M., Davis, J.M., Muga, S.J., and Carson, J.A. (2008). Interleukin-6 and cachexia in ApcMin/+ mice. Am. J. Physiol. Regul. Integr. Comp. Physiol. *294*, R393–R401.

Bonetto, A., Aydogdu, T., Kunzevitzky, N., Guttridge, D.C., Khuri, S., Koniaris, L.G., and Zimmers, T.A. (2011). STAT3 activation in skeletal muscle links muscle wasting and the acute phase response in cancer cachexia. PLoS ONE *6*, e22538.

Bradshaw, E.M., Raddassi, K., Elyaman, W., Orban, T., Gottlieb, P.A., Kent, S.C., and Hafler, D.A. (2009). Monocytes from patients with type 1 diabetes spontaneously secrete proinflammatory cytokines inducing Th17 cells. J. Immunol. *183*, 4432–4439.

Carrero, J.J., Chmielewski, M., Axelsson, J., Snaedal, S., Heimbürger, O., Bárány, P., Suliman, M.E., Lindholm, B., Stenvinkel, P., and Qureshi, A.R. (2008). Muscle atrophy, inflammation and clinical outcome in incident and prevalent dialysis patients. Clin. Nutr. *27*, 557–564.

Cheung, W.W., Paik, K.H., and Mak, R.H. (2010). Inflammation and cachexia in chronic kidney disease. Pediatr. Nephrol. *25*, 711–724.

Du, J., Wang, X., Miereles, C., Bailey, J.L., Debigare, R., Zheng, B., Price, S.R., and Mitch, W.E. (2004). Activation of caspase-3 is an initial step triggering accelerated muscle proteolysis in catabolic conditions. J. Clin. Invest. *113*, 115–123.

Feldman, B.J., Streeper, R.S., Farese, R.V., Jr., and Yamamoto, K.R. (2006). Myostatin modulates adipogenesis to generate adipocytes with favorable metabolic effects. Proc. Natl. Acad. Sci. USA *103*, 15675–15680.

Foss-Freitas, M.C., Foss, N.T., Donadi, E.A., and Foss, M.C. (2006). In vitro TNF-alpha and IL-6 production by adherent peripheral blood mononuclear cells obtained from type 1 and type 2 diabetic patients evaluated according to the metabolic control. Ann. N Y Acad. Sci. *1079*, 177–180.

Fouque, D., Kalantar-Zadeh, K., Kopple, J.D., Cano, N., Chauveau, P., Cuppari, L., Franch, H.A., Guarnieri, G., Ikizler, T.A., Kaysen, G.A., et al.

(2008). A proposed nomenclature and diagnostic criteria for protein-energy wasting in acute and chronic kidney disease. Kidney Int. *73*, 391–398.

Goodman, M.N. (1994). Interleukin-6 induces skeletal muscle protein breakdown in rats. Proc. Soc. Exp. Biol. Med. *205*, 182–185.

Gutiérrez, O.M., Mannstadt, M., Isakova, T., Rauh-Hain, J.A., Tamez, H., Shah, A., Smith, K., Lee, H., Thadhani, R., Jüppner, H., and Wolf, M. (2008). Fibroblast growth factor 23 and mortality among patients undergoing hemodialysis. N. Engl. J. Med. *359*, 584–592.

Hirano, T., Nakajima, K., and Hibi, M. (1997). Signaling mechanisms through gp130: a model of the cytokine system. Cytokine Growth Factor Rev. *8*, 241–252.

Horvath, C.M. (2004). The Jak-STAT pathway stimulated by interleukin 6. Sci. STKE *2004*, tr9.

Hu, Z., Wang, H., Lee, I.H., Du, J., and Mitch, W.E. (2009). Endogenous glucocorticoids and impaired insulin signaling are both required to stimulate muscle wasting under pathophysiological conditions in mice. J. Clin. Invest. *119*, 3059–3069.

Hung, A.M., Ellis, C.D., Shintani, A., Booker, C., and Ikizler, T.A. (2011). IL-1β receptor antagonist reduces inflammation in hemodialysis patients. J. Am. Soc. Nephrol. *22*, 437–442.

Kimmel, P.L., Phillips, T.M., Simmens, S.J., Peterson, R.A., Weihs, K.L., Alleyne, S., Cruz, I., Yanovski, J.A., and Veis, J.H. (1998). Immunologic function and survival in hemodialysis patients. Kidney Int. *54*, 236–244.

Kishimoto, T., Taga, T., and Akira, S. (1994). Cytokine signal transduction. Cell *76*, 253–262.

Lalani, R., Bhasin, S., Byhower, F., Tarnuzzer, R., Grant, M., Shen, R., Asa, S., Ezzat, S., and Gonzalez-Cadavid, N.F. (2000). Myostatin and insulin-like growth factor-I and -II expression in the muscle of rats exposed to the microgravity environment of the NeuroLab space shuttle flight. J. Endocrinol. *167*, 417–428.

Lecker, S.H., Jagoe, R.T., Gilbert, A., Gomes, M., Baracos, V., Bailey, J., Price, S.R., Mitch, W.E., and Goldberg, A.L. (2004). Multiple types of skeletal muscle atrophy involve a common program of changes in gene expression. FASEB J. *18*, 39–51.

Lecker, S.H., Goldberg, A.L., and Mitch, W.E. (2006). Protein degradation by the ubiquitin-proteasome pathway in normal and disease states. J. Am. Soc. Nephrol. *17*, 1807–1819.

Lee, S.W., Dai, G., Hu, Z., Wang, X., Du, J., and Mitch, W.E. (2004). Regulation of muscle protein degradation: coordinated control of apoptotic and ubiquitin-proteasome systems by phosphatidylinositol 3 kinase. J. Am. Soc. Nephrol. *15*, 1537–1545.

Ma, K., Mallidis, C., Artaza, J., Taylor, W., Gonzalez-Cadavid, N., and Bhasin, S. (2001). Characterization of 5′-regulatory region of human myostatin gene: regulation by dexamethasone in vitro. Am. J. Physiol. Endocrinol. Metab. *281*, E1128–E1136.

May, R.C., Kelly, R.A., and Mitch, W.E. (1987). Mechanisms for defects in muscle protein metabolism in rats with chronic uremia. Influence of metabolic acidosis. J. Clin. Invest. *79*, 1099–1103.

Myśliwiec, M., Balcerska, A., Zorena, K., Myśliwska, J., Lipska, B.S., Wiśniewski, P., and Myśliwski, A. (2006). Serum and urinary cytokine homeostasis and renal tubular function in children with type 1 diabetes mellitus. J. Pediatr. Endocrinol. Metab. *19*, 1421–1427.

Myśliwiec, M., Balcerska, A., Zorena, K., Myśliwska, J., Lipowski, P., and Raczyńska, K. (2008). The role of vascular endothelial growth factor, tumor necrosis factor alpha and interleukin-6 in pathogenesis of diabetic retinopathy. Diabetes Res. Clin. Pract. *79*, 141–146.

Okuma, Y., O'Connor, A.E., Muir, J.A., Stanton, P.G., de Kretser, D.M., and Hedger, M.P. (2005). Regulation of activin A and inhibin B secretion by inflammatory mediators in adult rat Sertoli cell cultures. J. Endocrinol. *187*, 125–134.

Penner, G., Gang, G., Sun, X., Wray, C., and Hasselgren, P.O. (2002). C/EBP DNA-binding activity is upregulated by a glucocorticoid-dependent mechanism in septic muscle. Am. J. Physiol. Regul. Integr. Comp. Physiol. *282*, R439–R444.

Poli, V. (1998). The role of C/EBP isoforms in the control of inflammatory and native immunity functions. J. Biol. Chem. *273*, 29279–29282.

Price, S.R., Bailey, J.L., Wang, X., Jurkovitz, C., England, B.K., Ding, X., Phillips, L.S., and Mitch, W.E. (1996). Muscle wasting in insulinopenic rats results from activation of the ATP-dependent, ubiquitin-proteasome proteolytic pathway by a mechanism including gene transcription. J. Clin. Invest. *98*, 1703–1708.

Ramji, D.P., and Foka, P. (2002). CCAAT/enhancer-binding proteins: structure, function and regulation. Biochem. J. *365*, 561–575.

Redell, M.S., Ruiz, M.J., Alonzo, T.A., Gerbing, R.B., and Tweardy, D.J. (2011). Stat3 signaling in acute myeloid leukemia: ligand-dependent and -independent activation and induction of apoptosis by a novel small-molecule Stat3 inhibitor. Blood *117*, 5701–5709.

Rui, L., Fisher, T.L., Thomas, J., and White, M.F. (2001). Regulation of insulin/insulin-like growth factor-1 signaling by proteasome-mediated degradation of insulin receptor substrate-2. J. Biol. Chem. *276*, 40362–40367.

Rui, L., Yuan, M., Frantz, D., Shoelson, S., and White, M.F. (2002). SOCS-1 and SOCS-3 block insulin signaling by ubiquitin-mediated degradation of IRS1 and IRS2. J. Biol. Chem. *277*, 42394–42398.

Ryba-Stanisławowska, M., Skrzypkowska, M., Myśliwska, J., and Myśliwiec, M. (2013). The serum IL-6 profile and Treg/Th17 peripheral cell populations in patients with type 1 diabetes. Mediators Inflamm. *2013*, 205284.

Sandri, M., Sandri, C., Gilbert, A., Skurk, C., Calabria, E., Picard, A., Walsh, K., Schiaffino, S., Lecker, S.H., and Goldberg, A.L. (2004). Foxo transcription factors induce the atrophy-related ubiquitin ligase atrogin-1 and cause skeletal muscle atrophy. Cell *117*, 399–412.

Sanford, D.C., and DeWille, J.W. (2005). C/EBPdelta is a downstream mediator of IL-6 induced growth inhibition of prostate cancer cells. Prostate *63*, 143–154.

Shelbaya, S., Amer, H., Seddik, S., Allah, A.A., Sabry, I.M., Mohamed, T., and El Mosely, M. (2012). Study of the role of interleukin-6 and highly sensitive C-reactive protein in diabetic nephropathy in type 1 diabetic patients. Eur. Rev. Med. Pharmacol. Sci. *16*, 176–182.

Sterneck, E., Paylor, R., Jackson-Lewis, V., Libbey, M., Przedborski, S., Tessarollo, L., Crawley, J.N., and Johnson, P.F. (1998). Selectively enhanced contextual fear conditioning in mice lacking the transcriptional regulator CCAAT/enhancer binding protein delta. Proc. Natl. Acad. Sci. USA *95*, 10908–10913.

Stitt, T.N., Drujan, D., Clarke, B.A., Panaro, F., Timofeyva, Y., Kline, W.O., Gonzalez, M., Yancopoulos, G.D., and Glass, D.J. (2004). The IGF-1/PI3K/Akt pathway prevents expression of muscle atrophy-induced ubiquitin ligases by inhibiting FOXO transcription factors. Mol. Cell *14*, 395–403.

Takeda, K., Kaisho, T., Yoshida, N., Takeda, J., Kishimoto, T., and Akira, S. (1998). Stat3 activation is responsible for IL-6-dependent T cell proliferation through preventing apoptosis: generation and characterization of T cell-specific Stat3-deficient mice. J. Immunol. *161*, 4652–4660.

Trendelenburg, A.U., Meyer, A., Rohner, D., Boyle, J., Hatakeyama, S., and Glass, D.J. (2009). Myostatin reduces Akt/TORC1/p70S6K signaling, inhibiting myoblast differentiation and myotube size. Am. J. Physiol. Cell Physiol. *296*, C1258–C1270.

Verzola, D., Procopio, V., Sofia, A., Villaggio, B., Tarroni, A., Bonanni, A., Mannucci, I., De Cian, F., Gianetta, E., Saffioti, S., and Garibotto, G. (2011). Apoptosis and myostatin mRNA are upregulated in the skeletal muscle of patients with chronic kidney disease. Kidney Int. *79*, 773–782.

Wang, X.H., Zhang, L., Mitch, W.E., LeDoux, J.M., Hu, J., and Du, J. (2010). Caspase-3 cleaves specific 19 S proteasome subunits in skeletal muscle stimulating proteasome activity. J. Biol. Chem. *285*, 21249–21257.

Xu, X., Kasembeli, M.M., Jiang, X., Tweardy, B.J., and Tweardy, D.J. (2009). Chemical probes that competitively and selectively inhibit Stat3 activation. PLoS ONE *4*, e4783.

Yang, H., Mammen, J., Wei, W., Menconi, M., Evenson, A., Fareed, M., Petkova, V., and Hasselgren, P.O. (2005). Expression and activity of

C/EBPbeta and delta are upregulated by dexamethasone in skeletal muscle. J. Cell. Physiol. *204*, 219–226.

Zhang, Y., Sif, S., and DeWille, J. (2007). The mouse C/EBPdelta gene promoter is regulated by STAT3 and Sp1 transcriptional activators, chromatin remodeling and c-Myc repression. J. Cell. Biochem. *102*, 1256–1270.

Zhang, L., Du, J., Hu, Z., Han, G., Delafontaine, P., Garcia, G., and Mitch, W.E. (2009). IL-6 and serum amyloid A synergy mediates angiotensin II-induced muscle wasting. J. Am. Soc. Nephrol. *20*, 604–612.

Zhang, L., Rajan, V., Lin, E., Hu, Z., Han, H.Q., Zhou, X., Song, Y., Min, H., Wang, X., Du, J., and Mitch, W.E. (2011). Pharmacological inhibition of myostatin suppresses systemic inflammation and muscle atrophy in mice with chronic kidney disease. FASEB J. *25*, 1653–1663.

Zhou, X., Wang, J.L., Lu, J., Song, Y., Kwak, K.S., Jiao, Q., Rosenfeld, R., Chen, Q., Boone, T., Simonet, W.S., et al. (2010). Reversal of cancer cachexia and muscle wasting by ActRIIB antagonism leads to prolonged survival. Cell *142*, 531–543.